European Radiology
https://doi.org/10.1007/s00330-019-06554-5

MUSCULOSKELETAL

MRI with state-of-the-art metal artifact reduction after total hip arthroplasty: periprosthetic findings in asymptomatic and symptomatic patients

Lukas Filli[1] · Pia M. Jungmann[1,2] · Patrick O. Zingg[3] · Hannes A. Rüdiger[4] · Julien Galley[1] · Reto Sutter[1] · Christian W. A. Pfirrmann[1]

Received: 14 June 2019 / Revised: 7 October 2019 / Accepted: 29 October 2019

Abstract

Objectives To assess the spectrum of periprosthetic MRI findings after primary total hip arthroplasty (THA).

Methods This multi-center cohort study analyzed 31 asymptomatic patients (65.7 ± 12.7 years) and 27 symptomatic patients (62.3 ± 11.9 years) between 6 months and 2 years after THA. 1.5-T MRI was performed using Compressed Sensing SEMAC and high-bandwidth sequences. Femoral stem and acetabular cup were assessed for bone marrow edema, osteolysis, and periosteal reaction in Gruen zones and DeLee and Charnley zones. Student *t* test and Fisher's exact test were performed.

Results The asymptomatic and symptomatic groups showed different patterns of imaging findings. Bone marrow edema was seen in 19/31 (61.3%) asymptomatic and 22/27 (81.5%) symptomatic patients, most commonly in Gruen zones 1, 7, and 8 ($p \geq 0.18$). Osteolysis occurred in 14/31 (45.2%) asymptomatic and 14/27 (51.9%) symptomatic patients and was significantly more common in Gruen zone 7 in the symptomatic group (8/27 (29.6%)) compared to the asymptomatic group (2/31 (6.5%)) ($p = 0.03$). Periosteal reaction was present in 4/31 asymptomatic (12.9%) and 9/27 symptomatic patients (33.3%) and more common in Gruen zones 5 and 6 in the symptomatic group ($p = 0.04$ and 0.02, respectively). In the acetabulum, bone marrow edema pattern was encountered in 3/27 (11.1%) symptomatic patients but not in asymptomatic patients ($p \geq 0.21$). Patient management was altered in 8/27 (29.6%) patients based on MRI findings.

Conclusions Periprosthetic bone marrow edema is common after THA both in asymptomatic and symptomatic patients. Osteolysis and periosteal reaction are more frequent in symptomatic patients. MRI findings led to altered patient management in 29.6% of patients.

Key Points

- *Bone marrow edema pattern was frequent in both asymptomatic and symptomatic patients after THA, particularly around the proximal femoral stem in Gruen zones 1, 7, and 8.*
- *Osteolysis was significantly more frequent in symptomatic patients in Gruen zone 7.*
- *Periosteal reaction occurred more frequently in symptomatic patients in Gruen zones 5 and 6.*

Keywords Magnetic resonance imaging · Hip · Arthroplasty · Artifact · Bone

✉ Lukas Filli
lukas.filli@balgrist.ch

[1] Radiology, Balgrist University Hospital, University of Zurich, Forchstrasse 340, CH-8008 Zurich, Switzerland

[2] Department of Diagnostic and Interventional Radiology, Medical Center - University of Freiburg, Faculty of Medicine, University of Freiburg, Freiburg, Germany

[3] Department of Orthopedic Surgery, Balgrist University Hospital, University of Zurich, Zurich, Switzerland

[4] Department of Orthopaedics, Schulthess Clinic, Zurich, Switzerland

Abbreviations

CS	Compressed sensing
ETL	Echo train length
FOV	Field of view
HASTE	Half-Fourier acquisition single-shot turbo spin echo
ICC	Intra-class correlation coefficient
NSA	Number of signal averages
OIP	Optimized inversion pulse
SEMAC	Slice encoding for metal artifact correction
SES	Slice encoding steps

Published online: 20 December 2019

STIR	Short τ inversion recovery
TA	Acquisition time
TE	Echo time
THA	Total hip arthroplasty
TI	Inversion time
TR	Repetition time
WOMAC	Western Ontario and McMaster Universities Arthritis Index

Introduction

The prevalence of total hip arthroplasty (THA) has grown significantly during the last decades, thereby increasing the demand for postoperative imaging [1]. Complications after THA include implant loosening, osteolysis, periprosthetic fracture, hardware failure, and infection [2–5]. Early detection of these complications is crucial to guide patient management and improve outcome [6].

Serial radiographs are helpful for evaluating the implant and adjacent bone after THA [7, 8] but cannot be used for assessing bone marrow and periprosthetic soft tissues [9]. However, bone marrow or soft tissue alterations may be the first indicators of postoperative complications [10]. Because MRI with metal artifact reduction techniques is the most accurate imaging method for these structures after THA [11–14], it is often performed in addition to radiographs and has become an inherent part of the routine postoperative workup at some institutions [15]. Advanced sequences such as Slice Encoding for Metal Artifact Correction (SEMAC) improve the detection of complications after THA [16–19]. While conventional SEMAC is limited by relatively long acquisition times [20, 21], the use of the recently introduced Compressed Sensing for SEMAC (CS-SEMAC) overcomes this limitation [22–24].

MRI protocols with advanced sequences for metal artifact reduction are now applicable to clinical routine and allow insights into periprosthetic processes. Early diagnosis of postoperative complications such as loosening or low-grade infection may lead to earlier revision surgery. As MRI is better than radiographs in detecting complications, it may alter patient management. Still, the radiological interpretation of MRI findings remains challenging because these are commonly encountered in asymptomatic individuals as well. For example, postoperative bone marrow edema pattern frequently occurs in the greater and lesser trochanter [1, 7]. To date, no systematic study has been performed on the prevalence and clinical relevance of such findings on MRI. Thus, the aim of the present study was to evaluate the frequency of different periprosthetic MRI findings in asymptomatic and symptomatic patients following primary THA by applying a state-of-the-art imaging protocol including CS-SEMAC.

Materials and methods

Study population

Ethical approval for this combined prospective-retrospective multi-center cohort study was obtained from the local ethics committee (Cantonal Ethics Committee, Zurich, BASEC ID 2016-02135). Written informed consent was obtained from all prospectively included asymptomatic subjects. Ethical approval for retrospective inclusion of symptomatic patients in both study centers (center 1: Balgrist University Hospital, Zurich, Switzerland; center 2: Schulthess Clinic, Zurich, Switzerland) was waived by the local ethics committee.

For the asymptomatic patient group, consecutive patients were recruited between January 2017 and March 2018 during their regular 12-month follow-up orthopedic consultation after THA at study center 1. Inclusion criteria were age ≥ 18 years, Western Ontario and McMaster Universities Arthritis Index (WOMAC) score ≤ 1 (considered "asymptomatic" [25, 26]) as well as oral and written informed consent to participate in the study. Exclusion criteria comprised general contraindications for MRI (e.g., cardiac pacemaker or cochlear implant), and revision surgery or complex surgery (cerclage wires, acetabular reinforcement or bone grafting, cement, tumor prosthesis) as well as known periprosthetic infection.

For the symptomatic patient group, all patients who underwent postoperative MRI after THA for clinical reasons between January 2017 and March 2018 were considered. Inclusion criteria were age ≥ 18 years, THA performed at one of the two study centers, postoperative hip pain warranting further workup with MRI (suspected muscular lesions, tendinopathy, loosening, bursitis, greater trochanteric pain syndrome, groin pain, or unspecified hip pain), and time interval between THA and postoperative MRI between 6 months and 2 years. Exclusion criteria were identical as for the asymptomatic patient group.

Imaging

Postoperative baseline and 12-month follow-up radiographs comprised a frontal (anteroposterior) view of the pelvis and a lateral cross-table view of the affected hip.

All patients from both study centers were scanned in the same 1.5-T MR scanner at center 1 (MAGNETOM Avanto Fit, Siemens Healthcare) using an 18-channel surface coil. All symptomatic and asymptomatic subjects underwent the same clinical MRI protocol optimized for metal artifact reduction around the hip prosthesis. Besides dedicated high-bandwidth sequences in all standard imaging planes, the protocol included an axial short τ inversion recovery (STIR) sequence with an optimized inversion pulse (STIR-OIP) and increased bandwidth as well as a dedicated coronal STIR CS-SEMAC sequence as part of a vendor-specific work-in-progress package

(Siemens Healthcare). The CS-SEMAC sequence was applied with 19 slice-encoding steps (SES), 10 iterations, and a normalization factor of 0.001 to achieve optimal image quality [24]. In order to measure the femoral torsion, an additional sequence was acquired over the ipsilateral knee. Detailed imaging parameters are listed in Table 1.

Image analysis

All radiographs and MRI datasets were assessed separately by two independent board-certified musculoskeletal radiologists blinded to clinical data (reader 1 and reader 2: C.W.A.P. and L.F., with 22 and 7 years of experience in musculoskeletal imaging, respectively).

On postoperative baseline radiographs, acetabular cup inclination and femoral stem alignment (varus/valgus) were determined using standardized measurements [27]. Twelve-month follow-up radiographs were compared to the baseline studies and assessed for the presence of secondary migration or subsidence as well as periprosthetic radiolucency. Radiolucency was separately evaluated in all Gruen zones around the femoral stem [28] and in all DeLee and Charnley zones around the acetabular cup [29] (Fig. 1).

On MRI, all Gruen zones and DeLee and Charnley zones were assessed for the presence of periprosthetic bone marrow edema pattern, osteolysis, and/or periosteal reaction. Bone marrow edema pattern was defined as STIR hyperintense signal in the bone [15, 30]. Periosteal reaction was defined as periosteal STIR hyperintensity. The amount of joint fluid and the capsular thickness was measured in four directions relative to the prosthesis (lateral, medial, anterior, posterior). Femoral torsion was calculated based on the standard transverse measurement method [31, 32].

Statistical analysis

Statistical analysis was performed using SPSS (v23, IBM Corp.) and Prism (v6, GraphPad). The inter-observer and intra-observer agreement were determined by calculating intra-class correlation coefficients (ICCs) (two-way, absolute agreement) for quantitative variables and Cohen's κ for qualitative variables, respectively. ICCs were interpreted according to Landis and Koch [33], and Cohen's κ according to Kundel and Polansky [34]. For the intra-observer agreement, reader 2 performed a second readout of 20 randomly selected subjects (9 asymptomatic, 11 symptomatic) with an interval of 12 months between the readouts.

Two-tailed Student *t* test was used to compare continuous variables between asymptomatic and symptomatic patients, whereas two-sided Fisher's exact test was used for binomial variables. Correlations between demographic and imaging variables were assessed with Spearman's ρ.

Results

Study population

Thirty-one asymptomatic patients agreed to participate in the study (20 males, 11 females; mean age, 65.7 ± 12.7 years; age range, 40–90 years), with mean a WOMAC score of 0.2 ± 0.3 (range, 0.0–1.0). Twenty-seven patients were included in the symptomatic group (12 males, 15 females; mean age, 62.3 ± 11.9 years; age range, 40–84 years). The flowchart of patient inclusion and exclusion is presented in Fig. 2. There was no known periprosthetic infection in both groups. Detailed demographic data are listed in Table 2.

Table 1 Detailed MRI protocol optimized for metal artifact reduction. *CS* = compressed sensing, *ETL* = echo train length, *FOV* = field of view, *HASTE* = half-Fourier acquisition single-shot turbo spin echo, *NSA* = number of signal averages, *SEMAC* = slice encoding for metal artifact correction, *STIR* = short τ inversion recovery, *OIP* = Optimized Inversion Pulse, *TA* = acquisition time, *TE* = echo time, *TR* = repetition time

Parameter	Coronal STIR CS-SEMAC	Axial STIR OIP	Coronal T2 high bandwidth	Axial T1 high bandwidth	Sagittal T1 high bandwidth	T2 HASTE (knee)
TR/TE (ms)	4220/36	4000/31	4000/58	669/8.6	627/7.3	1400/93
ETL	9	11	15	3	3	154
NSA	1	3	2	2	2	1
Number of slices	25	27	20	29	31	10
Section thickness (mm)	4	7	4	6	4	5
Spacing (mm)	4	8.75	6	8.4	4.4	6.5
Matrix	256 × 205	384 × 269	512 × 282	512 × 410	320 × 320	256 × 256
FOV (mm^2)	280 × 280	189 × 189	220 × 220	210 × 210	200 × 200	240 × 240
Bandwidth (Hz/pixel)	500	450	390	425	435	700
slice encoding steps	19	–	–	–	–	–
TA (min:s)	06:19	03:56	02:28	02:17	01:59	00:54

All prostheses were cementless titanium-based systems with screwless acetabular cups and polyethylene inlays, and all were implanted via the anterior approach. Various implants were used in both groups as follows: Pinnacle® Hip Solutions (n = 8; DePuy Synthes, Johnson & Johnson), Versafitcup® and Quadra® System (n = 23; Medacta), R3™ Acetabular System and Polarstem™ (n = 13; Smith & Nephew), April Cup and Harmony® Stem System (n = 6; SymBios), and Fitmore® (n = 8; Zimmer Biomet).

All radiographs and MRI examinations were successfully performed. The mean interval between THA and postoperative MRI was 390 ± 14 days in the asymptomatic group (range, 359–418 days) and 417 ± 172 days in the symptomatic group (range, 190–725 days) (p = 0.38). In one asymptomatic patient, the knee sequence was not acquired, which precluded femoral torsion measurement in this subject.

Inter-observer agreement

Regarding measurements on radiographs, inter-observer agreement was "good" for acetabular cup inclination (ICC = 0.86, 95% CI 0.77–0.92) and femoral stem alignment (ICC = 0.71, 95% CI 0.51–0.83), "substantial" for osteolysis (κ = 0.72), and "moderate" for femoral stem subsidence (κ = 0.53). Concerning MR imaging findings, inter-observer agreement was "good" for femoral torsion (ICC = 0.88, 95% CI 0.79–0.93); "substantial" for bone marrow edema pattern (κ = 0.63), osteolysis (κ = 0.73), joint fluid (κ = 0.65), and capsular thickness (κ = 0.77); and "moderate" for periosteal reaction (κ = 0.57).

Intra-observer agreement

Intra-observer agreement was "good" for acetabular cup inclination (ICC = 0.88, 95% CI 0.68–0.95) and femoral stem alignment (ICC = 0.72, 95% CI 0.32–0.89) and "moderate" for osteolysis (κ = 0.55) and femoral stem subsidence (κ = 0.59). For MRI findings, intra-observer agreement was "almost perfect" for femoral torsion (ICC = 0.95, 95% = 0.86–0.98), "substantial" for bone marrow edema pattern (κ = 0.63) and osteolysis (κ = 0.67) and "moderate" for capsular thickness (κ = 0.59), joint fluid (κ = 0.56), and periosteal reaction (κ = 0.59).

Measurements and frequency of findings on radiographs

Acetabular cup inclination was 37.7 ± 5.5° (range 28–51°) (reader 2: 37.6 ± 5.7°, range 28–51°) in asymptomatic patients and 40.7 ± 4.6° (33–51°) (reader 2: 39.7 ± 5.1°, range 29–51°) in symptomatic patients. Mean femoral stem alignment was 1.6° varus ± 1.7° (range between 0° and 8° varus) (reader 2:

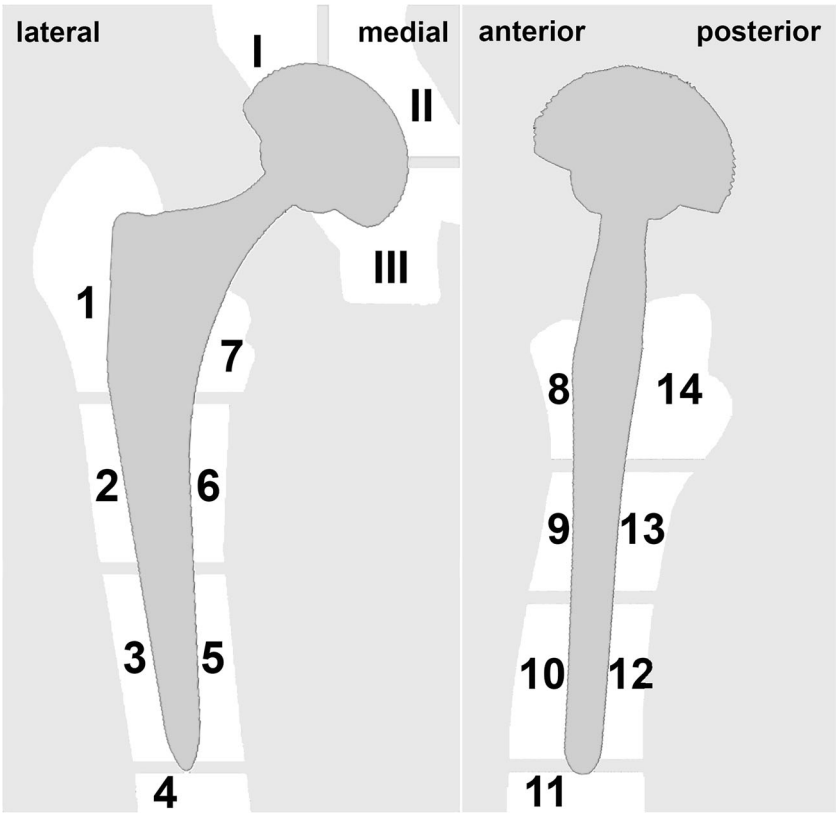

Fig. 1 Schematic drawing of different zones around the femoral stem (Gruen zones 1–14) and the acetabular cup (DeLee & Charnley zones I–III). Gruen zones 4 and 11 represent the same anatomical location but on different projections

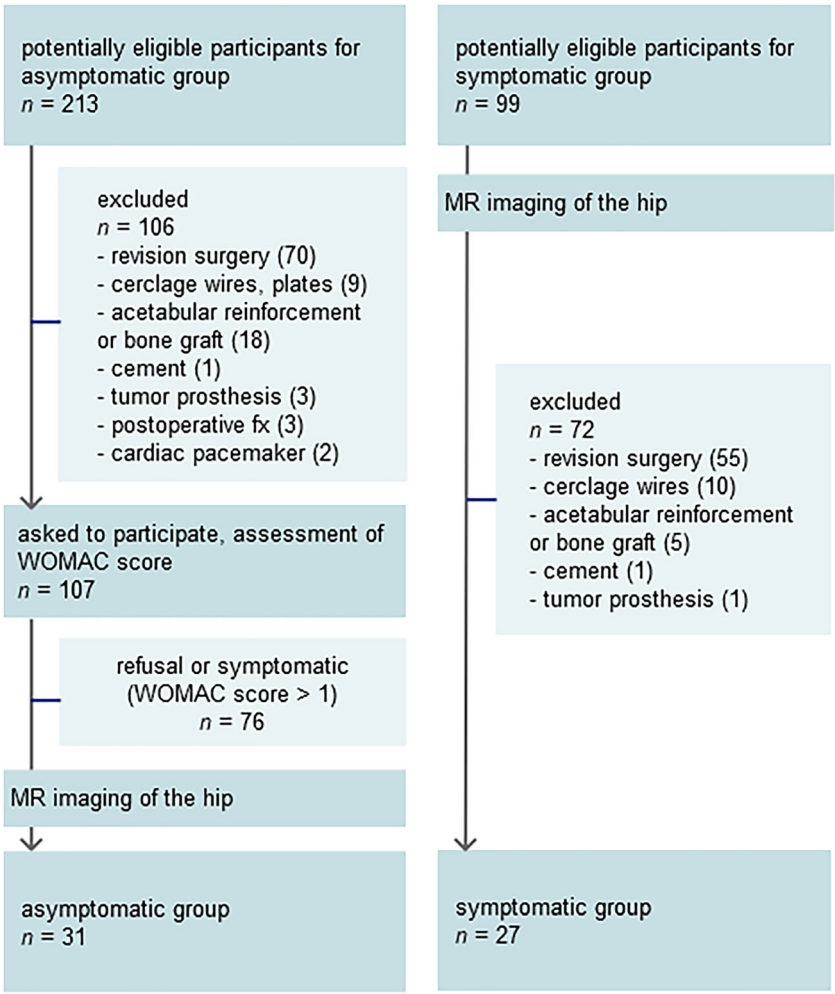

Fig. 2 Flowchart of patient inclusion and exclusion for the asymptomatic group (prospective analysis) and symptomatic group (retrospective analysis) of patients with primary uncemented THA. Both groups were scanned with the same MRI protocol

1.1° varus ± 1.8°, range between 6° varus and 3° valgus) in asymptomatic patients and 1.4° varus ± 1.5° (range between 4° varus and 3° valgus) (reader 2: 0.4° varus ± 1.4°, range between 4° varus and 3° valgus) in symptomatic patients. On 12-month follow-up radiographs, subsidence of femoral stem was observed by both readers in 5/31 (16.1%) asymptomatic and 1/27 (3.7%) symptomatic patients, with an amount of 1.7 ± 0.8 mm (1–3 mm) in these six patients. Apart from radiolucent lines, no postoperative complications (e.g., periprosthetic fracture) were observed on radiography.

Table 2 Demographic data of the two study groups. Unless otherwise indicated, data are ± standard deviation and data in parentheses are range. *THA* = total hip arthroplasty, *WOMAC* = Western Ontario and McMaster Universities Arthritis Index questionnaire

Parameter	Both groups (n = 58)	Asymptomatic group (n = 31)	Symptomatic group (n = 27)	p value
Mean age (year)	64.4 ± 12.4 (40–90)	65.7 ± 12.7 (40–90)	62.3 ± 11.9 (40–84)	0.29
Sex				0.19
No. of men	32	20	12	
No. of women	26	11	15	
No. of examinations per side				0.18
Left	24	10	14	
Right	34	21	13	
Mean interval between THA and MRI (day)	404 ± 118 (190–725)	390 ± 14 (359–418)	417 ± 172 (190–725)	0.38
WOMAC score	–	0.2 ± 0.3 (0.0–1.0)	–	–

Measurements and frequency of MRI findings

Bone marrow edema pattern and osteolysis were commonly encountered in both asymptomatic and symptomatic patients, particularly around the proximal femur in Gruen zones 1, 7, and 8 (examples in Figs. 3 and 4). Detailed results for all Gruen zones and DeLee and Charnley zones regarding bone marrow edema pattern, osteolysis, and periosteal reaction are presented in Figs. 5 and 6 (reader 1 and 2, respectively). Joint fluid was most pronounced in the medial aspect, measuring > 6 mm in 24/31 (77.4%) of asymptomatic patients (reader 2: equal results) and in 21/27 (77.7%) of symptomatic patients (reader 2: 19/27, 70.4%) (Table 3). In both the asymptomatic and symptomatic group, the capsule was thickest in the anterior and lateral aspects (Table 4).

Femoral antetorsion was 17 ± 10° (range − 2 to 31°) (reader 2: 17 ± 9°, range 3 to 34°) in asymptomatic and 15 ± 10° (range − 12 to 38°) (reader 2: 15 ± 7°, range 2–27°) in symptomatic patients.

Whereas 39/70 (55.7%) of osteolytic Gruen zones were visible both on radiographs and MRI, 28/70 (40.0%) were visible on MRI only and 3/70 (4.3%) on radiographs only (Table 5). On MRI, 8/67 (11.9%) of osteolytic zones measured > 2 mm in width and were observed in Gruen zones 1 (n = 5), 6 (n = 1), and 7 (n = 2).

Statistical comparison and correlations

No significant differences were found between asymptomatic and symptomatic patients regarding acetabular cup inclination (reader 1: p = 0.57; reader 2: p = 0.15), femoral stem alignment (reader 1: p = 0.12; reader 2: p = 0.16), femoral torsion (reader 1: p = 0.52; reader 2: p = 0.19), subsidence of the femoral stem (both readers: p = 0.20) or osteolysis on 12-month follow-up radiographs (reader 1: p = 0.21–1.0 depending on Gruen and DeLee and Charnley zones; reader 2: p = 0.20–1.0 accordingly). At MRI, both readers observed osteolysis more frequently in Gruen zone 7 in the symptomatic group (p = 0.03 for reader 1 and p = 0.006 for reader 2, respectively). For the symptomatic group, reader 1 additionally observed significantly more frequent osteolysis in Gruen zone 6 (p = 0.002), and bone marrow edema pattern in Gruen zone 14 (p = 0.03) as well as periosteal reaction in Gruen zones 5 (p = 0.04) and 6 (p = 0.02). No significant differences were found regarding osteolysis in the other zones (p = 0.39–1.0), bone marrow edema pattern (p = 0.18–1.0), periosteal reaction (p = 0.20–1.0), amount of joint fluid (p = 0.11–1.0) or capsular thickness (p = 0.47–1.0) in both readouts.

No significant correlation was found regarding the occurrence of bone marrow edema pattern, osteolysis, and periosteal reaction in relation to age, sex, acetabular cup inclination, stem alignment, femoral torsion, or subsidence of the femoral stem ($p \geq 0.07$). There was a weak positive correlation between the presence of osteolysis and bone marrow edema pattern (Spearman's ρ = 0.13, $p < 0.001$). Strong positive correlation was found between osteolysis visible on radiographs and osteolysis visible on MRI (Spearman's ρ = 0.72, $p < 0.001$).

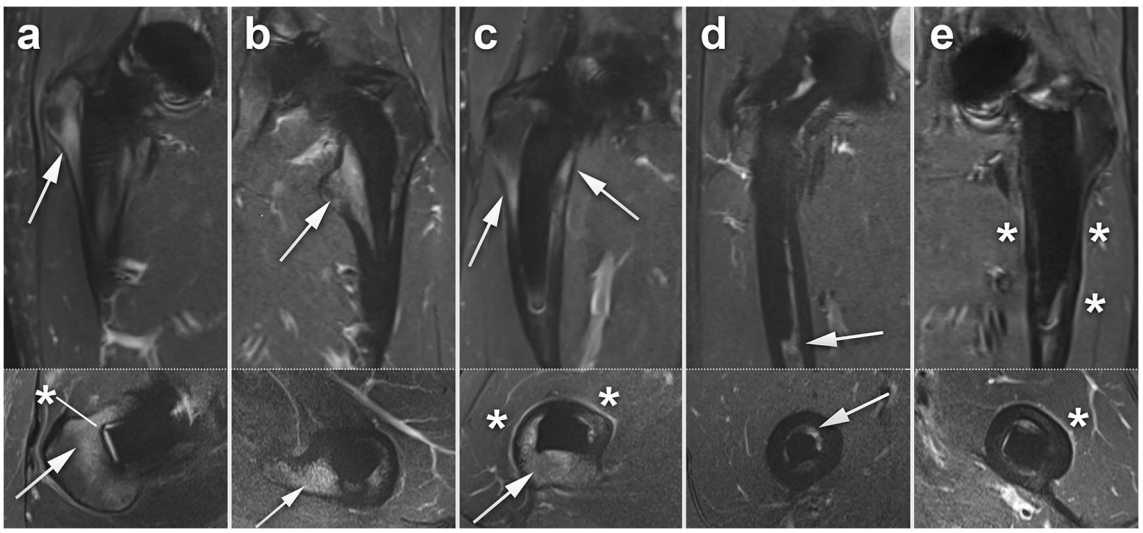

Fig. 3 Imaging findings on coronal STIR CS-SEMAC MRI (upper row) and axial STIR-OIP (lower row) in different patients one year after THA. **a** 52-year-old asymptomatic female with laterally predominant bone marrow edema pattern around the proximal stem (arrows). Also note the narrow osteolysis anterior and lateral to the proximal shaft (asterisk). **b** 56-year-old symptomatic male with medially predominant bone marrow edema pattern around the proximal stem (arrows). **c** 67-year-old asymptomatic male with bone marrow edema pattern predominant around the middle third of the femoral stem (arrows). Periosteal reaction is present in the anterior and lateral aspect of the femoral shaft (asterisks). **d** 61-year-old symptomatic male with bone marrow edema pattern medial to the distal third of the femoral shaft (arrows). **e** 63-year-old symptomatic female patient showing semicircular periosteal reaction around the femoral shaft (asterisks)

Indications for MRI and working diagnosis in symptomatic patients

All symptomatic patients presented with postoperative hip pain. The working diagnosis before MRI in these patients comprised suspected muscular lesions or tendinopathy (10/27, 37.0%), suspected loosening (4/27, 14.8%), suspected bursitis (4/27, 14.8%)), suspected greater trochanteric pain syndrome (7/27, 25.9%), and pain of unclear origin (2/27, 7.4%). Final working diagnoses after MRI and orthopedic consultation included muscular pain in 4/27 (14.8%), abductor tendinopathy in 5/27 (18.5%), iliopsoas bursitis in 1/27 (3.7%), failed ingrowth or fibrous tissue ingrowth in 2/27 (7.4%; subsequent revision in one patient with intraoperative confirmation of loosening, no revision so far in the other patient), and unclear pain in 8/27 (29.6%), whereas pain spontaneously resolved in 7/27 (25.9%). In the patient with intraoperatively confirmed stem loosening, MRI before revision surgery exhibited bone marrow edema pattern in Gruen zones 1, 4, 7, 8, 11, and 14 as well as osteolysis in Gruen zones 1 (> 2 mm), 7 (1 mm), 8 (> 2 mm), and 14 (1 mm). By changing the working diagnosis, MRI altered patient management in 8/27 (29.6%) of patients.

Discussion

In the present multi-center study on MRI after THA, periprosthetic bone marrow edema was common in both symptomatic and asymptomatic patients. Although osteolysis and periosteal reaction were more common in symptomatic patients, no specific pattern of imaging findings was identified for reliable differentiation between asymptomatic and symptomatic patients.

MRI findings such as extensive bone marrow edema, osteolysis, and or periosteal reaction, particularly in combination with joint fluid and soft tissue alterations, warrant further diagnostic workup for potential periprosthetic infection. This may ultimately lead to earlier diagnosis and revision surgery and potentially improve patient outcome. Thus, MRI is a useful tool to detect postoperative complications potentially missed on conventional radiographs.

The increasing prevalence of THA and the use of higher field strengths have increased the demand for reliable metal artifact reduction at MRI. This is best achieved through a combination of high-bandwidth sequences and advanced techniques such as SEMAC [16, 17], MAVRIC, or hybrid sequences [21, 35]. However, SEMAC is limited by a trade-off between artifact reduction and acquisition time, as the latter linearly increases with the number of SES. The "optimal" number of SES depends on the type of implant material. The widespread titanium-based implants, which were investigated in the presents study, are paramagnetic and increase the local magnetic field only moderately. In contrast, ferromagnetic materials such as cobalt-chromium and stainless steel lead to more pronounced artifacts [36]. In an experimental work on different THA at 1.5 T, a minimum of 5 SES was required for titanium prostheses, 9 SES for cobalt-chromium, and 13 SES for stainless steel [37]. However, higher numbers

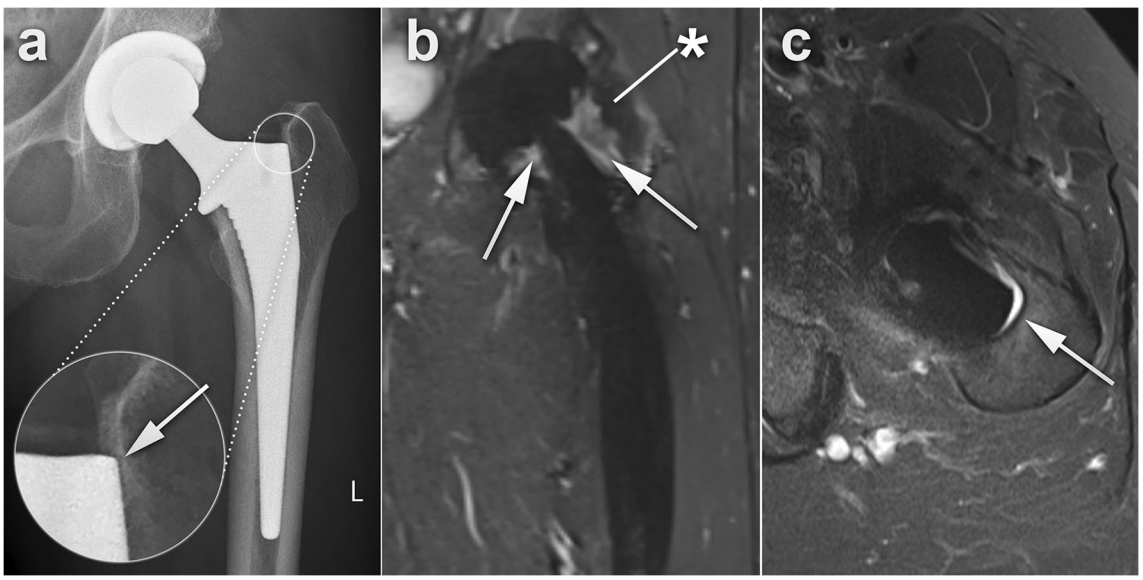

Fig. 4 53-year-old female patient from the symptomatic group 8 months after uncemented primary total hip arthroplasty via anterior approach. MRI was performed because the patient suffered from diffuse postoperative hip pain. **a** On anteroposterior radiographic view, a small lucency in Gruen zone 1 is depicted (arrow). No subsidence of the femoral stem occurred compared to the baseline radiograph (not shown). **b** Coronal STIR CS-SEMAC MRI reveals moderate amounts of joint fluid (arrows) and a thick lateral joint capsule (asterisk). **c** On axial STIR-OIP, osteolysis with fluid signal intensity is seen in Gruen zones 1 and 8 (arrow)

of SES would be desirable, as subtle periprosthetic findings can still be obscured by metal artifacts even with 9 SES [10].

CS-SEMAC allows accelerated imaging by using pseudo-random k-space undersampling and iterative reconstruction [22]. The higher efficiency gained from this technique allows additional SES while preserving clinically feasible acquisition times. In recent feasibility studies, 15 to 19 SES have been applied for imaging of total hip and knee arthroplasties in order to maximize visualization of periprosthetic structures [23, 24, 38]. In the present work, a state-of-the-art MRI protocol including a STIR CS-SEMAC sequence with 19 SES has been used for MRI after THA. This allowed detailed assessment of periprosthetic processes in asymptomatic and symptomatic patients.

Bone marrow edema pattern after THA can result from reactive changes after intraoperative reaming and broaching but also from mechanical stress reaction or infection [15, 39] and is best evaluated on STIR images [7]. STIR is the method of choice for fat suppression around metal because it is relatively insensitive to magnetic field inhomogeneities [6, 15, 17, 40]. The combination of coronal STIR CS-SEMAC and an axial STIR sequence with optimized inversion pulse and high bandwidth in our study allowed excellent depiction of all Gruen zones (Fig. 3). Bone marrow edema pattern was commonly encountered in the greater and lesser trochanter (Gruen zones 1 and 7, respectively) but less frequent in more distal Gruen zones (Figs. 5 and 6). This distribution pattern may be explained by the higher amount of trabecular bone in these zones compared to more distal Gruen zones. The findings are in line with a previous study, which reported bone marrow edema pattern in the greater and lesser trochanter in 6/15 symptomatic hips (40%) after THA [7].

Uncemented THA are designed with structured surfaces to facilitate bone ingrowth [4]. Nevertheless, a frequent phenomenon in uncemented THA is the development of a fibrous membrane, likely as a reaction to mechanical stress. This limits osseous integration and may progress to implant loosening [8, 15, 41]. On MRI, fibrous membrane formation manifests as increased signal intensity at the bone-implant interface [6] and is best visualized with advanced techniques such

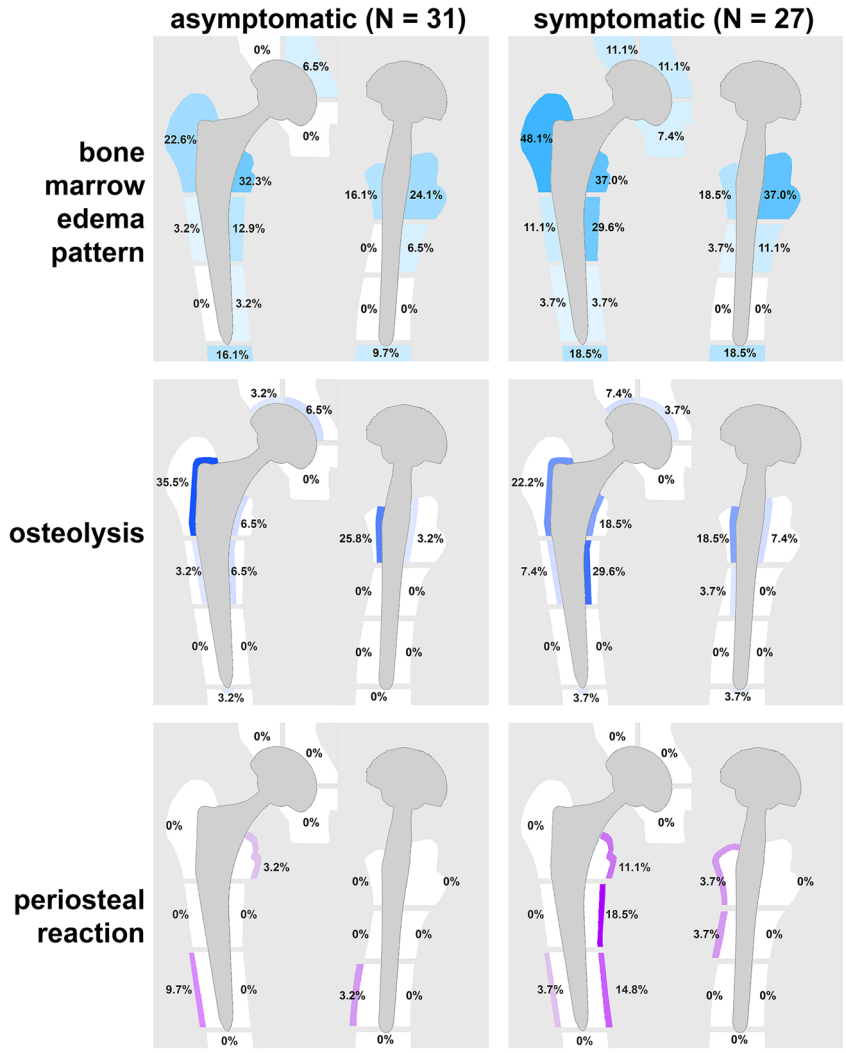

Fig. 5 Schematic illustration of the frequencies of bone marrow edema pattern, osteolysis, and periosteal reaction in asymptomatic and symptomatic patients (data from reader 1). The frequencies of different findings are indicated by different color intensities and listed as percentages. Bone marrow edema pattern was most commonly found in Gruen zones 1, 6, and 7 in both groups, whereas osteolysis predominantly occurred around the proximal third of the femoral stem, i.e., in Gruen zones 1, 7, 8, and 14. Periosteal reaction was most commonly noted in Gruen zones 5–7 in symptomatic patients

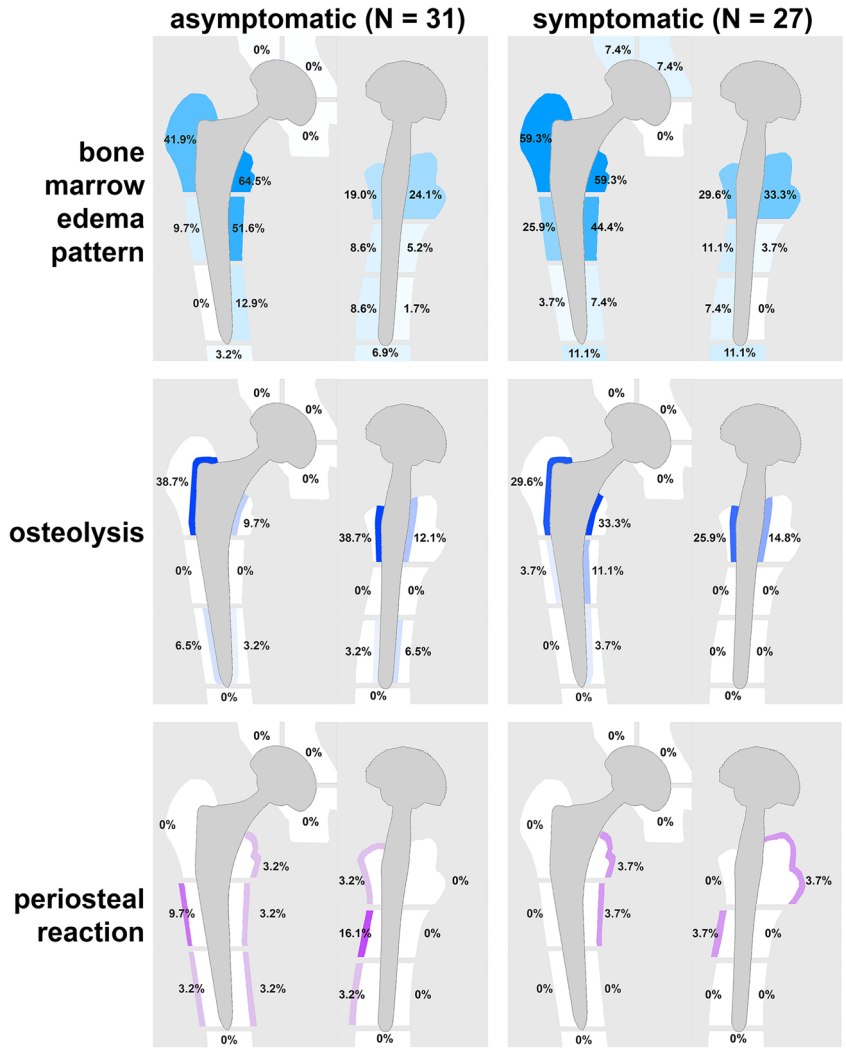

Fig. 6 Schematic illustration of the frequencies of bone marrow edema pattern, osteolysis, and periosteal reaction in asymptomatic and symptomatic patients (data from reader 2). The frequencies of different findings are indicated by different color intensities and listed as percentages. Bone marrow edema pattern was most commonly found in Gruen zones 1, 6, and 7 in both groups, whereas osteolysis predominantly occurred around the proximal third of the femoral stem, i.e., in Gruen zones 1, 7, 8, and 14. Periosteal reaction most commonly appeared in Gruen zone 9 in asymptomatic patients

as STIR SEMAC [17, 38]. The clinical relevance of a thin STIR hyperintense layer remains unclear, because it does not necessarily indicate loosening [42] and was frequently found in completely asymptomatic patients in the present study.

Table 3 Amount of joint fluid, measured as the distance between the prosthetic head and the joint capsule in four directions (anterior, lateral, posterior, medial). In both asymptomatic and symptomatic subjects, joint fluid was most pronounced in the medial aspect

		Asymptomatic group (n = 31)		Symptomatic group (n = 27)	
		Reader 1	Reader 2	Reader 1	Reader 2
Anterior	< 3 mm	28 (90.3%)	29 (93.5%)	20 (74.1%)	18 (66.7%)
	3–6 mm	1 (3.2%)	0	4 (14.8%)	3 (11.1%)
	> 6 mm	2 (6.5%)	2 (6.5%)	3 (11.1%)	6 (22.2%)
Lateral	< 3 mm	21 (67.7%)	17 (54.9%)	18 (66.7%)	11 (40.7%)
	3–6 mm	6 (19.4%)	5 (16.1%)	3 (11.1%)	5 (18.6%)
	> 6 mm	4 (12.9%)	9 (29.0%)	6 (22.2%)	11 (40.7%)
Posterior	< 3 mm	29 (93.5%)	30 (96.8%)	25 (92.6%)	24 (88.9%)
	3–6 mm	2 (6.5%)	0	2 (7.4%)	2 (7.4%)
	> 6 mm	0	1 (3.2%)	0	1 (3.7%)
Medial	< 3 mm	5 (16.1%)	6 (19.4%)	2 (7.4%)	4 (14.8%)
	3–6 mm	2 (6.5%)	1 (3.2%)	4 (14.8%)	4 (14.8%)
	> 6 mm	24 (77.4%)	24 (77.4%)	21 (77.7%)	19 (70.4%)

Table 4 Capsular thickness measured in four directions. In both asymptomatic and symptomatic patients, the capsule was thickest in the anterior and lateral aspects

		Asymptomatic group (n = 31)		Symptomatic group (n = 27)	
		Reader 1	Reader 2	Reader 1	Reader 2
Anterior	< 3 mm	0	1 (3.2%)	5 (18.5%)	1 (3.7%)
	3–6 mm	3 (9.7%)	2 (6.5%)	1 (3.7%)	2 (7.4%)
	> 6 mm	28 (90.3%)	28 (90.3%)	21 (77.7%)	24 (88.9%)
Lateral	< 3 mm	2 (6.5%)	2 (6.5%)	4 (14.8%)	2 (7.4%)
	3–6 mm	2 (6.5%)	0	1 (3.7%)	1 (3.7%)
	> 6 mm	27 (87.1%)	29 (93.6%)	22 (81.5%)	24 (88.9%)
Posterior	< 3 mm	30 (96.8%)	22 (71.0%)	26 (96.3%)	20 (74.1%)
	3–6 mm	1 (3.2%)	5 (16.1%)	1 (3.7%)	3 (11.1%)
	> 6 mm	0	4 (12.9%)	0	4 (14.8%)
Medial	< 3 mm	31 (100%)	29 (93.6%)	27 (100%)	25 (92.6%)
	3–6 mm	0	1 (3.2%)	0	1 (3.7%)
	> 6 mm	0	1 (3.2%)	0	1 (3.7%)

Some authors measure the thickness of the hyperintense layer to differentiate between fibrous membrane formation (layer 1–2 mm) and bone resorption (layer > 2 mm) [8, 15]. In the present study, STIR hyperintensity was termed "osteolysis" regardless of its thickness. Loosening should not be confounded with secondary subsidence of the femoral stem, which is common in uncemented implants within the first postoperative year [8] and was found in 10.3% (6/58) of patients in our study.

Periosteal reaction (defined as hyperintensity on STIR images) can be a manifestation of osseous stress reaction [15] (Fig. 3). In the present study, periosteal reaction was more common in symptomatic patients (Fig. 5 and 6). Hence, the presence of focal periosteal reaction after THA seems to be a clinically significant finding.

Bone marrow edema pattern in the acetabulum was assessed by using DeLee and Charnley zones, which were initially introduced for radiographs (Fig. 1). These zones do not account for the three-dimensional architecture of the acetabulum and potential differences between the anterior and posterior parts. However, bone marrow edema pattern in the acetabulum was a relatively rare finding in our study. Postoperative edema needs to be differentiated from preexisting degenerative subchondral cysts in the acetabular roof not resected during surgery.

In asymptomatic and symptomatic patients, the anterior and lateral capsule was commonly thick (> 6 mm) likely due to postoperative scarring (Fig. 4). Therefore, this finding should not be overinterpreted in the setting of unclear hip pain. In most patients, only little joint fluid was present (radius

Table 5 Frequency and distribution of osteolysis in different Gruen zones as depicted on radiographs and MRI. MRI was more sensitive than radiographs, particularly in Gruen zone 8

Gruen zone	Osteolysis visible on radiographs and MRI	Osteolysis visible on MRI only	Osteolysis visible on radiographs only
1	15	5	1
2	1	0	0
3	0	0	0
4	0	0	0
5	0	3	0
6	1	3	1
7	5	5	0
8	10	9	0
9	0	0	0
10	1	1	0
11	0	0	0
12	1	0	0
13	0	0	0
14	5	2	1
Total (zones 1–14)	39 (55.7%)	28 (40.0%)	3 (4.3%)

< 3 mm in all directions). The presence of higher amounts of joint fluid with or without capsular distension may warrant further workup for potential periprosthetic infection.

There are limitations to our study. First, the cross-sectional study design precludes evaluation of the predictive value of MRI findings in terms of future complications such as implant loosening. Second, this study was limited to primary uncemented THA, and all patients received titanium-based systems; our observations may not apply for complex surgery, revision surgery, cemented prostheses, or ferromagnetic implant types. Third, implants of different vendors were evaluated, which however reflects the situation in daily clinical routine, and minor differences in design seem negligible. Fourth, soft tissue alterations, which are a common source of postoperative hip pain, were not systematically evaluated because the present study focused on juxtaprosthetic MRI findings. Last, there was no reference standard (such as intraoperative confirmation) for the occurrence of osteolysis as seen on radiographs and MRI.

In conclusion, various MRI findings are prevalent in asymptomatic patients after THA, in particular periprosthetic bone marrow edema pattern. Although osteolysis and periosteal reaction are more frequent in symptomatic patients, the overlap of MRI findings between asymptomatic and symptomatic patients does not allow to identify a specific pattern of findings which is always associated with symptoms. The imaging findings are readily depicted by using a state-of-the art MRI protocol including CS-SEMAC.

Funding information The authors state that this work has not received any funding.

Compliance with ethical standards

Guarantor The scientific guarantor of this publication is Lukas Filli.

Conflict of interest The authors of this manuscript declare no relationships with any companies whose products or services may be related to the subject matter of the article.

Statistics and biometry No complex statistical methods were necessary for this paper.

Informed consent Written informed consent was obtained from all prospectively included asymptomatic subjects in this study. Ethical approval for retrospective inclusion of symptomatic patients was waived by the local ethics committee.

Ethical approval Institutional Review Board approval was obtained.

Methodology
- Prospective
- Cross-sectional study
- Multi-center study

References

1. Burge AJ (2015) Total hip arthroplasty: MR imaging of complications unrelated to metal wear. Semin Musculoskelet Radiol 19:31–39
2. White LM, Kim JK, Mehta M et al (2000) Complications of total hip arthroplasty: MR imaging-initial experience. Radiology 215: 254–262
3. Del Pozo JL, Patel R (2009) Clinical practice. Infection associated with prosthetic joints. N Engl J Med 361:787–794
4. Roth TD, Maertz NA, Parr JA, Buckwalter KA, Choplin RH (2012) CT of the hip prosthesis: appearance of components, fixation, and complications. Radiographics 32:1089–1107
5. Mulcahy H, Chew FS (2012) Current concepts of hip arthroplasty for radiologists: part 2, revisions and complications. AJR Am J Roentgenol 199:570–580
6. Hayter CL, Koff MF, Potter HG (2012) Magnetic resonance imaging of the postoperative hip. J Magn Reson Imaging 35:1013–1025
7. Toms AP, Marshall TJ, Cahir J et al (2008) MRI of early symptomatic metal-on-metal total hip arthroplasty: a retrospective review of radiological findings in 20 hips. Clin Radiol 63:49–58
8. Chang CY, Huang AJ, Palmer WE (2015) Radiographic evaluation of hip implants. Semin Musculoskelet Radiol 19:12–20
9. Czerny C, Krestan C, Imhof H, Trattnig S (1999) Magnetic resonance imaging of the postoperative hip. Top Magn Reson Imaging 10:214–220
10. Otazo R, Nittka M, Bruno M et al (2016) Sparse-SEMAC: rapid and improved SEMAC metal implant imaging using SPARSE-SENSE acceleration. Magn Reson Med. https://doi.org/10.1002/mrm.26342
11. Potter HG, Foo LF (2006) Magnetic resonance imaging of joint arthroplasty. Orthop Clin North Am 37(361-373):vi–vii
12. Weiland DE, Walde TA, Leung SB et al (2005) Magnetic resonance imaging in the evaluation of periprosthetic acetabular osteolysis: a cadaveric study. J Orthop Res 23:713–719
13. Walde TA, Weiland DE, Leung SB et al (2005) Comparison of CT, MRI, and radiographs in assessing pelvic osteolysis: a cadaveric study. Clin Orthop Relat Res:138–144
14. Pfirrmann CW, Notzli HP, Dora C, Hodler J, Zanetti M (2005) Abductor tendons and muscles assessed at MR imaging after total hip arthroplasty in asymptomatic and symptomatic patients. Radiology 235:969–976
15. Fritz J, Lurie B, Miller TT, Potter HG (2014) MR imaging of hip arthroplasty implants. Radiographics 34:E106–E132
16. Lu W, Pauly KB, Gold GE, Pauly JM, Hargreaves BA (2009) SEMAC: slice encoding for metal artifact correction in MRI. Magn Reson Med 62:66–76
17. Sutter R, Ulbrich EJ, Jellus V, Nittka M, Pfirrmann CW (2012) Reduction of metal artifacts in patients with total hip arthroplasty with slice-encoding metal artifact correction and view-angle tilting MR imaging. Radiology 265:204–214
18. Khodarahmi I, Nittka M, Fritz J (2017) Leaps in technology: advanced MR imaging after total hip arthroplasty. Semin Musculoskelet Radiol 21:604–615
19. Jungmann PM, Agten CA, Pfirrmann CW, Sutter R (2017) Advances in MRI around metal. J Magn Reson Imaging 46:972–991
20. Hargreaves BA, Worters PW, Pauly KB, Pauly JM, Koch KM, Gold GE (2011) Metal-induced artifacts in MRI. AJR Am J Roentgenol 197:547–555
21. Koch KM, Brau AC, Chen W et al (2011) Imaging near metal with a MAVRIC-SEMAC hybrid. Magn Reson Med 65:71–82
22. Fritz J, Ahlawat S, Demehri S et al (2016) Compressed Sensing SEMAC: 8-fold accelerated high resolution metal artifact reduction

MRI of cobalt-chromium knee arthroplasty implants. Invest Radiol 51:666–676
23. Otazo R, Nittka M, Bruno M et al (2017) Sparse-SEMAC: rapid and improved SEMAC metal implant imaging using SPARSE-SENSE acceleration. Magn Reson Med 78:79–87
24. Jungmann PM, Bensler S, Zingg P, Fritz B, Pfirrmann CW, Sutter R (2019) Improved visualization of juxtaprosthetic tissue using metal artifact reduction magnetic resonance imaging: experimental and clinical optimization of Compressed Sensing SEMAC. Invest Radiol 54:23–31
25. Kim CO, Dietrich TJ, Zingg PO, Dora C, Pfirrmann CWA, Sutter R (2017) Arthroscopic hip surgery: frequency of postoperative MR arthrographic findings in asymptomatic and symptomatic patients. Radiology 283:779–788
26. Bellamy N, Buchanan WW, Goldsmith CH, Campbell J, Stitt LW (1988) Validation study of WOMAC: a health status instrument for measuring clinically important patient relevant outcomes to anti-rheumatic drug therapy in patients with osteoarthritis of the hip or knee. J Rheumatol 15:1833–1840
27. Johnston RC, Fitzgerald RH Jr, Harris WH, Poss R, Muller ME, Sledge CB (1990) Clinical and radiographic evaluation of total hip replacement. A standard system of terminology for reporting results. J Bone Joint Surg Am 72:161–168
28. Gruen TA, McNeice GM, Amstutz HC (1979) "Modes of failure" of cemented stem-type femoral components: a radiographic analysis of loosening. Clin Orthop Relat Res (141):17–27
29. DeLee JG, Charnley J (1976) Radiological demarcation of cemented sockets in total hip replacement. Clin Orthop Relat Res: 20–32
30. Zanetti M, Bruder E, Romero J, Hodler J (2000) Bone marrow edema pattern in osteoarthritic knees: correlation between MR imaging and histologic findings. Radiology 215:835–840
31. Sutter R, Dietrich TJ, Zingg PO, Pfirrmann CW (2015) Assessment of femoral antetorsion with MRI: comparison of oblique measurements to standard transverse measurements. AJR Am J Roentgenol 205:130–135
32. Sutter R, Dietrich TJ, Zingg PO, Pfirrmann CW (2012) Femoral antetorsion: comparing asymptomatic volunteers and patients with femoroacetabular impingement. Radiology 263:475–483
33. Landis JR, Koch GG (1977) The measurement of observer agreement for categorical data. Biometrics 33:159–174
34. Kundel HL, Polansky M (2003) Measurement of observer agreement. Radiology 228:303–308
35. Choi SJ, Koch KM, Hargreaves BA, Stevens KJ, Gold GE (2015) Metal artifact reduction with MAVRIC SL at 3-T MRI in patients with hip arthroplasty. AJR Am J Roentgenol 204:140–147
36. Filli L, Jud L, Luechinger R et al (2017) Material-dependent implant artifact reduction using SEMAC-VAT and MAVRIC: a prospective MRI phantom study. Invest Radiol 52:381–387
37. Deligianni X, Bieri O, Elke R, Wischer T, Egelhof T (2015) Optimization of scan time in MRI for total hip prostheses: SEMAC tailoring for prosthetic implants containing different types of metals. Rofo 187:1116–1122
38. Fritz J, Fritz B, Thawait GK et al (2016) Advanced metal artifact reduction MRI of metal-on-metal hip resurfacing arthroplasty implants: compressed sensing acceleration enables the time-neutral use of SEMAC. Skeletal Radiol 45:1345–1356
39. Mulcahy H, Chew FS (2012) Current concepts of hip arthroplasty for radiologists: part 1, features and radiographic assessment. AJR Am J Roentgenol 199:559–569
40. Del Grande F, Santini F, Herzka DA et al (2014) Fat-suppression techniques for 3-T MR imaging of the musculoskeletal system. Radiographics 34:217–233
41. Bosetti M, Masse A, Navone R, Cannas M (2001) Biochemical and histological evaluation of human synovial-like membrane around failed total hip replacement prostheses during in vitro mechanical loading. J Mater Sci Mater Med 12:693–698
42. Sugimoto H, Hirose I, Miyaoka E et al (2003) Low-field-strength MR imaging of failed hip arthroplasty: association of femoral periprosthetic signal intensity with radiographic, surgical, and pathologic findings. Radiology 229:718–723